ISSN 0967-0912, Steel in Translation, 2020, Vol. 50, No. 2, pp. 77–83. © Allerton Press, Inc., 2020.
Russian Text © The Author(s), 2020, published in Izvestiya Vysshikh Uchebnykh Zavedenii, Chernaya Metallurgiya, 2020, No. 2, pp. 108–115.

The Structural Formation in Differentially-Hardened 100-Meter-Long Rails during Long-Term Operation

V. E. Kormyshev[a, *], E. V. Polevoi[b, **], A. A. Yur'ev[b], V. E. Gromov[a, *], and Yu. F. Ivanov[c, ****]**

[a]*Siberian State Industrial University, Novokuznetsk, Kemerovo ~~oblast~~, 654007 Russia*
[b]*JSC Evraz United West Siberian Metallurgical Plant, Novokuznetsk, Kemerovo oblast, 654043 Russia*
[c]*Institute of High Current Electronics, SB RAS, Tomsk, 634055 Russia*
**e-mail: 89239230000@mail.ru*
***e-mail: Egor.Polevoj@evraz.com*
****e-mail: gromov@physics.sibsiu.ru*
*****e-mail: yufi55@mail.ru*

Received September 12, 2019; revised October 23, 2019; accepted November 15, 2019

Abstract—By using modern physical-materials science methods, the roll surface of structural-phase states and mechanical properties has been analyzed at a distance ranging from 0 to 22 mm with respect to the central axis and to the fillet of differentially-quenched DT 350 grade 100-meter-long rails. These rails have been manufactured at Evraz United West Siberian Metallurgical Plant after long-term operation on an experimental test ring (passed gross tonnage amounting to 1411 million tons). According to chemical composition, the rail metal satisfies the requirements of TU (Engineering Specifications) 0921-276–01124323–2012 for steel E76HF grade steel. The impact strength and hardness on the head's roll surface and throughout the cross section meet the TU (Engineering Specifications) requirements. The microstructure of the rail metal is represented by finely dispersed lamellar pearlite—1.5 points of scale No. 7 according to GOST (State Standard) 8233—with inclusions of excess ferrite along the grain boundaries. The interlamellar distance in the railhead ranges from 0.10 to 0.15 μm. The long-term operation of the rails is accompanied by the formation of a gradient structure presented by a regular change in hardness, microhardness, and impact strength throughout the railhead section. The microhardness at a depth of 2 mm counted from the roll surface amounts to 1481–1486 MPa. At a depth of 10 mm, the microhardness decreases to 1210–1385 MPa, which is caused by an increase in the interlamellar distance and by a decrease in the level of metal cold-work strengthening in the course of long-term operation. It has been suggested that this could be caused by an increase in the interlamellar distance and by a decrease in the level of cold-work strengthening in the course of long-term operation.

Keywords: structure, hardness, microhardness, differentially quenched rails, long-term operation

DOI: 10.3103/S0967091220020047

INTRODUCTION

Currently, the most widely-used methods in the production of long-length rails consist in differential quenching. These modern methods are devoid of the disadvantages inherent in bulk quenching [1]. The problem of the evolution of the structure and properties of rails in the course of long-term operation represents a complex set of interrelated scientific and technical issues. One of the most important directions in the development of ideas concerning the nature of structural-phase transformations consists in revealing quantitative structural regularities throughout the rail section.

Under current conditions of high ~~axle~~ loads and speeds, the rail surface layers experience intense plastic deformation in the course of long-term operation, which leads to damage. This could cause the removal of the rails [2]. The analysis of [3–8] shows that even at a relatively small run-off (gross operation amount ranging from 100 to 500 million tons), the rail surface layers exhibit the formation of structural-phase states with an anomalously high microhardness level and with a small grain size (ranging from 20 to 500 nm).

The cementite lamels are either bent or destroyed, extremely high dislocation density is observed at the interfacial boundaries, and cementite dissolution and austenite formation occur due to the reverse $\gamma \rightarrow \alpha$ transformation. Under the intense deformation impact during long-term operation, a set of different processes can occur (recrystallization, relaxation, phase transitions, phase decomposition and formation, amorphization, etc.), which can lead to the evolution of structural-and- phase states, as well as leading to a change (degradation) in the mechanical properties.

Table 1. Chemical composition of DT350 grade rails made of E76KhF steel

<table>
<tr><th rowspan="2">Material</th><th colspan="11">Content of chemical elements, %</th></tr>
<tr><th>C</th><th>Mn</th><th>Si</th><th>p</th><th>S</th><th>Cr</th><th>Ni</th><th>Cu</th><th>V</th><th>Al</th><th>Ti</th></tr>
<tr><td>Testing</td><td>0.72</td><td>0.77</td><td>0.61</td><td>0.010</td><td>0.009</td><td>0.42</td><td>0.07</td><td>0.14</td><td>0.038</td><td>0.003</td><td>0.003</td></tr>
<tr><td rowspan="2">TU (Engineering Specifications) requirements 0921-276-01124323–2012</td><td rowspan="2">0.71–0.82</td><td rowspan="2">0.75–1.25</td><td rowspan="2">0.25–0.60</td><td colspan="2">at most</td><td rowspan="2">0.20–0.80</td><td colspan="2">Σ at most0.27</td><td rowspan="2">0.030–0.150</td><td colspan="2">at most</td></tr>
<tr><td>0.020</td><td>0.020</td><td>0.20</td><td>0.20</td><td>0.004</td><td>0.025</td></tr>
</table>

In recent years, issues connected with the wear of rails during operation are covered in detail [9–17]. The wear and contact fatigue defects have much in common: both of them are initially formed in the surface layers [18]. As noted by the authors of [18], when rail metal has an increased hardness, the wear level is lower. The thickness of the plastically deformed layer is lower as well. High wear rates cause the contact fatigue to decrease by removing surface cracks. It is important to note that the onset of constant wear level coincides with the accumulation of plastic deformation [19]. It is natural that such a conclusion considers the relationship between the values of hardness in the wheel–rail system [20], as well as the structural-phase condition and chemical composition.

This work was aimed at analyzing the structure and properties of differentially quenched 100-meter-long rails during long-term operation.

MATERIALS AND METHODS

For materials under study, samples of 100-meter-long differentially quenched DT350 grade rails made of E76HF grade evacuated steel were used. These were taken from an experimental training range railway at Shcherbinka City after the passed gross tonnage amounted to 1411 million tons. The chemical compositions of the rail fragment under study are given in Table 1. According to chemical composition, the rail sample metal meets the requirements of TU (Engineering Specifications) 0921-276–01124323–2012 for the DT350 grade rails.

The metal macrostructure was revealed by deep etching in a 50% hot aqueous hydrochloric acid solution on an incomplete transverse template (head, neck). The macrostructure assessment was carried out in accordance with an RD 14-2R-5–2004 Classifier of macrostructure defects in rails rolled based on continuous cast billets of electric-furnace steel [21]. The metal microstructure was studied using thin sections cut from the top of the head (the fillet and the roll surface) before and after etching in a 4% alcoholic solution of nitric acid. The steel structure was studied by optical microscopy using an Olympus GX 51 microscope and by scanning electron microscopy using a Tescan MIRA 3 electron microscope.

The impact steel strength was determined for two samples of the first type cut from the railhead according to GOST (State Standard) 9454 at a testing temperature of +20°C. The hardness was measured using the Brinell and Rockwell method on the roll surface and throughout the head's cross section in accordance with the requirements of TU (Engineering Specifications) 0921-276–01124323–2012. In addition, the hardness was measured in the neck's upper part (about 30 mm above point 6 indicated in the requirements of point 1.8.1 in TU (Engineering Specifications) 0921-276–01124323-2012), as well as throughout the head's cross section in the transverse direction at a distance of 2, 10, and 22 mm counted from the railhead roll surface along the vertical symmetry axis, as well as from the fillets. The microhardness was determined using a PMT-3 unit using the Vickers method at an indenter load amounting to 300 mN at a distance of 2 and 10 mm from the surface at both fillets and the central zone of the sample head's roll surface based on the results of four measurements in each zone.

RESULTS AND DISCUSSION

Visually, the head's roll surface of a rail sample has a smooth and shiny appearance, with some wear shifting to one of the fillets. In the working fillet zone, there are cracks inherent in contact fatigue arranged almost at right angles to the rolling axis, alongside with small crumbling areas.

The metal macrostructure of the fragment under study is evaluated quite well according to the amount of axial segregation, point heterogeneity, segregation strips and cracks. Internal defects, as well as discontinuities on the template, were not found.

Near the roll surface, a darker etching area is observed, in which the formation is associated with metal deformation processes during long-term operation.

Near the working fillet surface in the surface crack zone inherent in contact fatigue, the optical microscopy of etched sections cut from the sample head has shown furcated discontinuities that penetrate to a depth of 1.09 mm at an acute angle to the surface (Fig. 1). The rail metal etching in the discontinuity zone has made it possible to reveal a structure with a high level of cold-work strengthening (see Fig. 2).

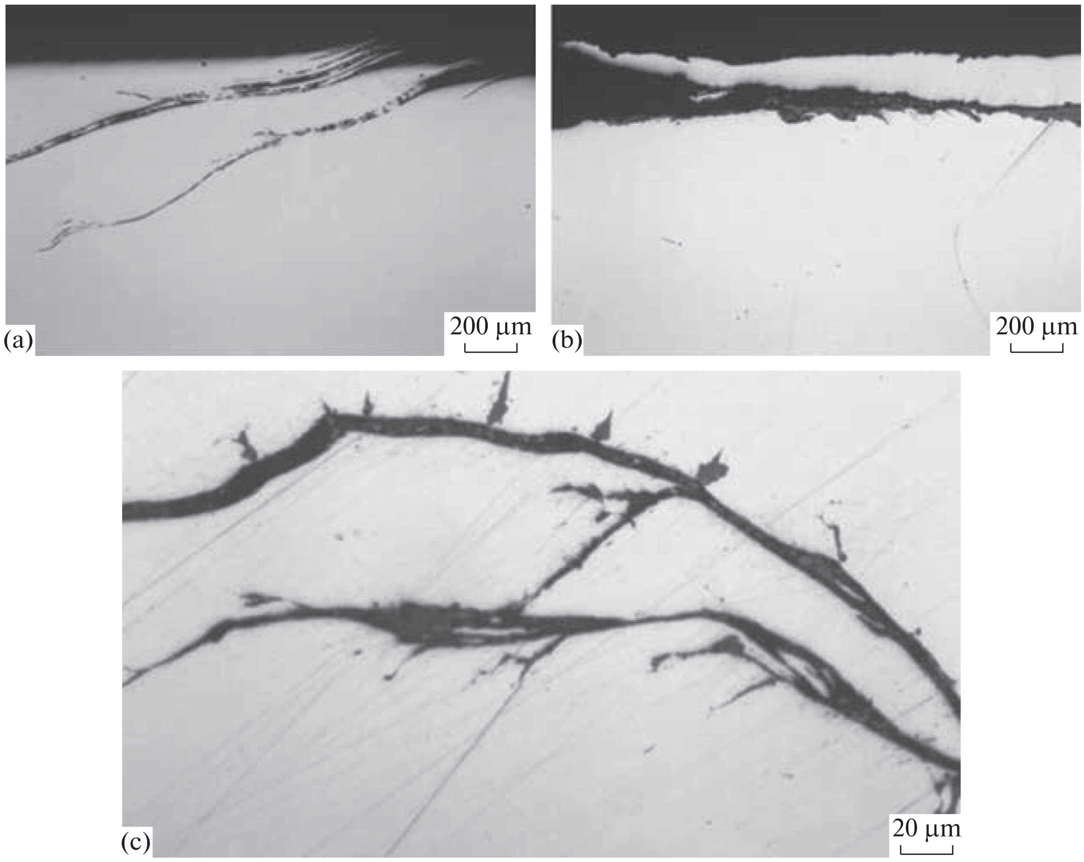

Fig. 1. Furcated discontinuities revealed in the railhead at the working fillet's surface at the place of contact fatigue surface cracks (optical microscopy of unetched thin sections).

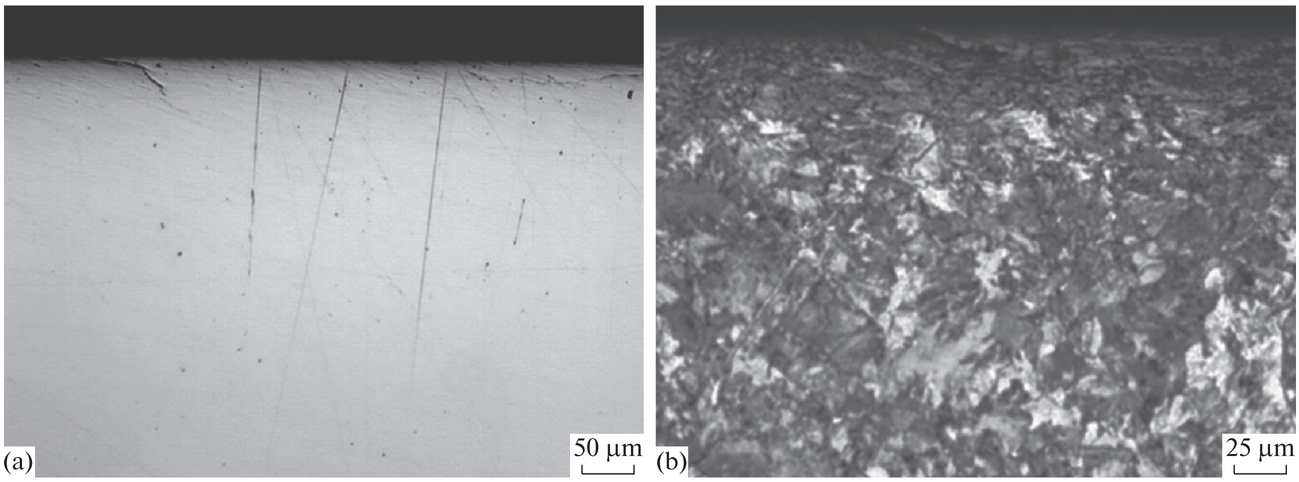

Fig. 2. Rail metal structure in the zone of furcated discontinuity revealed in the railhead fragment on the working fillet's surface at the place of surface cracks inherent in contact fatigue (optical microscopy of etched thin sections).

On thin sections cut from the railhead roll surface, there are single small discontinuities up to 0.03 mm deep (Fig. 3a). The deformation depth counted from the roll surface is negligible and amounts to 0.035 mm (Fig. 3b).

The microstructure in the sample head represents finely dispersed lamellar pearlite with fine inclusions of excess ferrite (1.5 points of scale No. 7 according to GOST (State Standard) 8233 (Figs. 4a, 4b). Bainite has not been observed in the sample metal micro-

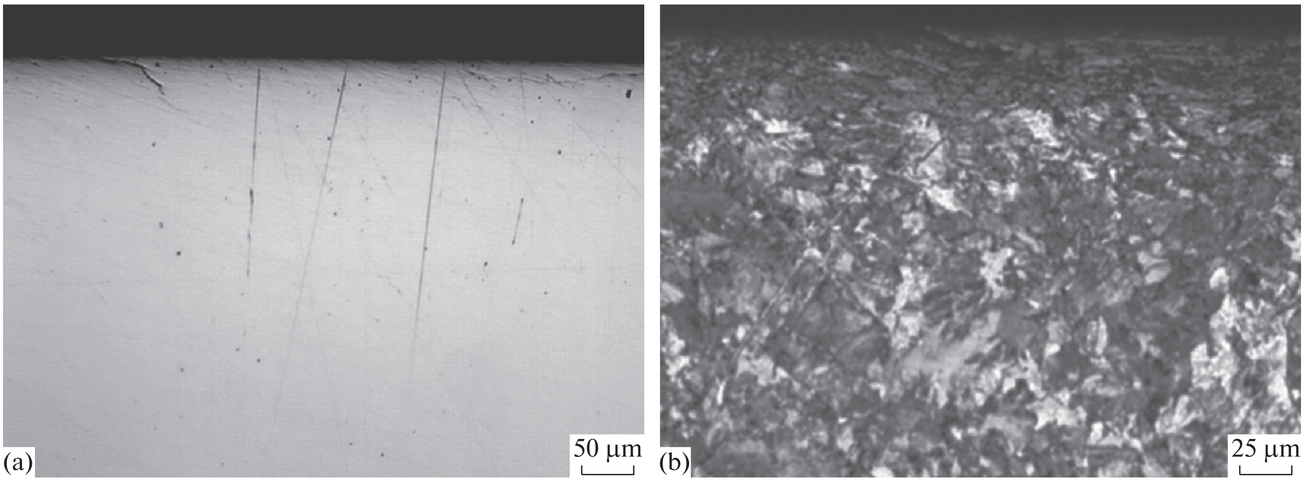

Fig. 3. Metal structure on the railhead roll surface. Optical microscopy images: (a) for unetched thin section, and (b) for etched thin section.

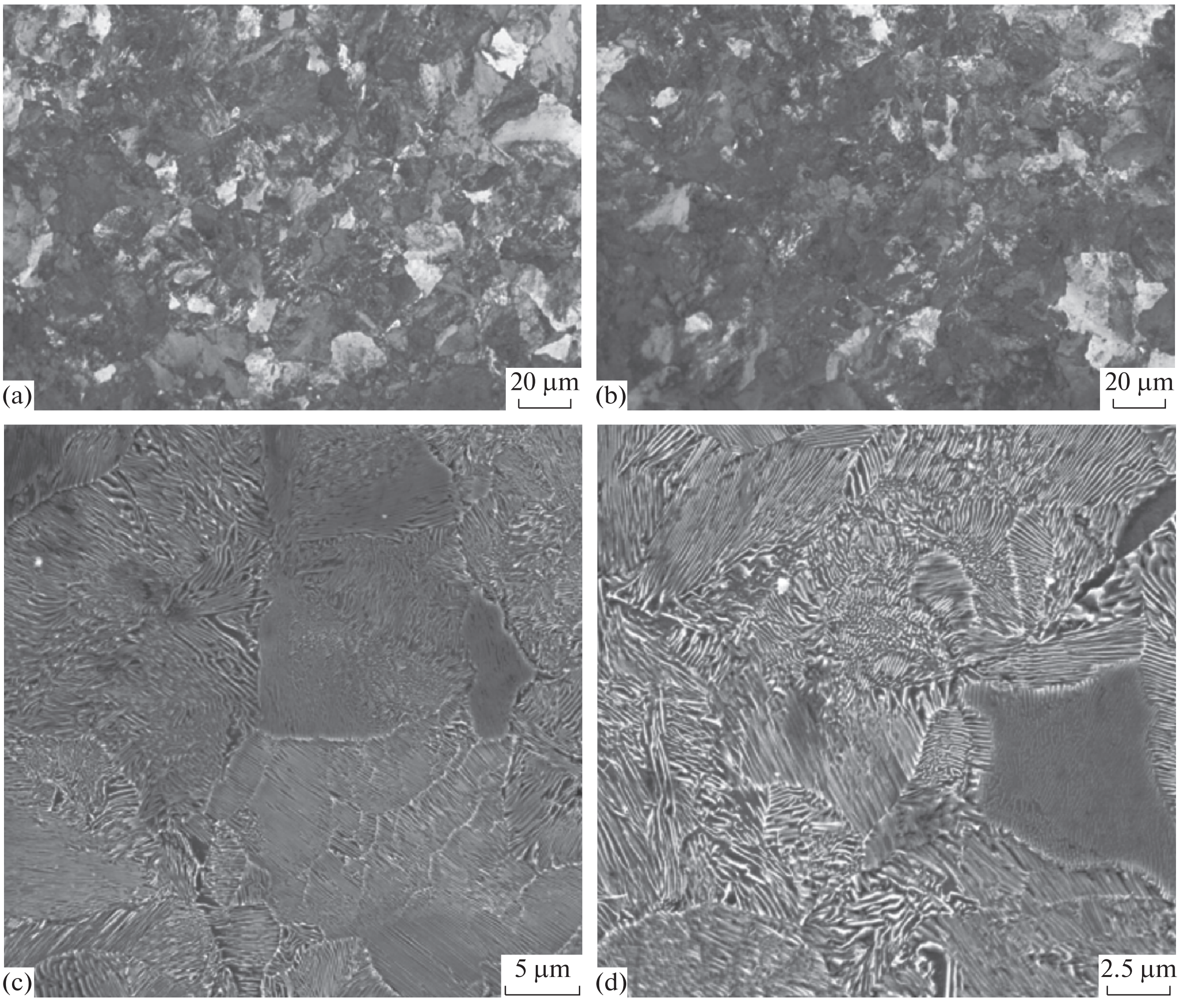

Fig. 4. Metal structure in the railhead, (a, b) revealed by optical microscopy, and (c, d) revealed by scanning electron microscopy for etched thin sections at a depth of 0.5–1.0 mm.

Table 2. Quantitative characteristics of railhead metal structure revealed in etched thin sections by optical and scanning electron microscopy

Sampling place	Interlamellar distance, μm			Size of pearlite clusters, μm			Grain diameter, μm (grain number)		
	min	max	medium	min	max	medium	min	max	medium
Fillet	0.073	0.256	0.132	2.711	12.157	6.170	15.042	51.169	29.800
Roll surface	0.073	0.225	0.125	2.634	10.731	5.600	–	–	–

Table 3. Impact strength and hardness of steel on the railhead roll surface (*HRS*) and throughout its cross section, as well as in the neck's upper part

Material	*KCU* +20°C, J/cm^2		Hardness *HB* at a distance of, mm					
			HRS	fillet	fillet		22	neck
					no. 1	no. 2		
~~@Проба рельса~~	30	27	388 399	381	364	362	373	345
Requirements of TU (Engineering Specifications) 0921-276–01124323–2012 for DT350 grade rails	at least 15		363–401	at least 341				at most 341

structure. The metal microstructure is represented by highly dispersed pearlite with small areas of structurally free ferrite occurring (Fig. 4c). In the pearlite structure, alongside with the regular clusters (with regularly arranged cementite lamels), there are many clusters with destroyed cementite lamels (Fig. 4d). In addition, some degenerate pearlite zones are observed.

The quantitative assessment results of the microstructure are presented in Table 2. Upon analysis of the results, a more dispersed pearlite structure inherent in the roll surface as compared with the pearlite structure in the fillet is observed.

The mechanical properties of steel have been characterized by impact strength, hardness and microhardness. The test results are given in Table 3. According to impact strength and hardness on the railhead roll surface and throughout its cross section, the tested metal samples meet the requirements of TU (Engineering Specifications) 0921-276–01124323–2012 for DT350 grade rails. The hardness measured in the neck is slightly increased as compared with the technical condition requirements.

In addition, measurements of the sample metal's hardness has been performed throughout the railhead cross section in the transverse direction using the Rockwell method at a distance of 2, 10 and 22 mm from the railhead roll surface along the vertical symmetry axis, as well as from the fillets (see Table 4).

The analysis of the results presented in Table 4 shows that the hardness at a depth of 2 mm in the central zone and in the working fillet zone is higher (38.5–37.1 HRC) as compared with the idle fillet hardness (35.3 HRC), which could be caused by deformation occurring in this zone, as well as cold-work strengthening of the material. At a depth of 10 and 22 mm counted from the roll surface, the metal hardness is 2–3 HRC lower as compared with the hardness at a depth of 2 mm and exhibits comparable values amounting to 34.8–35.8 HRC.

Table 5 presents the averaged (results of four measurements in each zone) microhardness values deter-

Table 4. Metal hardness throughout the railhead cross section in the transverse direction

Place of measurement	Hardness *HRC* at a distance from the surface, mm		
	2	10	22
Working fillet	38.5	35.5	34.8
Central zone	37.1	35.8	35.6
Idle fillet~~выкружка~~	35.3	35.5	35.2

Table 5. Rail microhardness at a distance of 2 and 10 mm from the surface at both fillets and the central zone of the roll surface

Measurement zone	Microhardness, MPa, at a distance from the surface, mm	
	2	10
Working fillet	1475	1385
Idle fillet	1486	1274
Roll surface	1481	1210

mined at a distance of 2 and 10 mm from the roll surface at the place of both fillets, as well as from the central zone of the railhead roll surface. The microhardness at a depth of 2 mm exhibits the values close to each other ranging within 1481–1475 MPa.

At a depth of 10 mm, the microhardness exhibits a decrease to 1210–1385 MPa, which could be a consequence of increasing the interlamellar distance (i.e., decreasing dispersion level) and a consequence of decreasing the cold-work strengthening level during long-term operation.

CONCLUSIONS

By using the methods of modern physical materials science, the impact strength and hardness on the railhead roll surface and throughout its cross section satisfy the requirements of TU (Engineering Specifications) 0921-276–01124323–2012 for DT350 grade rails. The hardness measured using the Rockwell method at a depth of 2 mm from the surface is 38.5–37.1 HRC, at a depth of 10 and 22 mm, this value amounts to 35.5–35.8 HRC and 34.8–35.6 HRC, respectively. The metal microstructure within the rails is represented by finely dispersed lamellar pearlite—1.5 points of scale No. 7 according to GOST (State Standard) 8233—with the inclusions of excess ferrite along the grain boundaries.

Bainite is not detected in the rail metal microstructure. The value of the interlamellar distance in the railhead ranges from 0.10 to 0.15 μm. The average size of pearlite clusters in the fillet zone amounts to 6.2 μm, whereas this parameter on the roll surface amounts to 5.6 μm. The main array of actual grain size, estimated only for the idle fillet zone, corresponds to number 7 according to GOST (State Standard) 5639–82. The microhardness at a depth of 2 mm counted from the roll surface amounts to 1481–1486 MPa.

At a depth of 10 mm, the microhardness decreases to 1210–1385 MPa, which is caused by an increase in the interlamellar distance, as well as by a decrease in the level of metal cold-work strengthening upon the long-term rail operation.

ACKNOWLEDGMENTS

The authors are grateful to A.M. Yunusov for his help in performing the experiments and discussing the results.

FUNDING

This work was financially supported by the Russian Foundation for Basic Research (project No. 19-32-60001).

REFERENCES

1. Gromov, V.E., Yuriev, A.B., Morozov, K.V., and Ivanov, Y.F., *Microstructure of Quenched Rails*, Cambridge: Cambridge Int. Sci., 2016.
2. Shur, E.A., *Povrezhdeniya rel'sov* (Rail Damage), Moscow: Intekst, 2012.
3. Ivanisenko, Yu. and Fecht, H.J., Microstructure modification in the surface layers of railway rails and wheels, *Steel Tech.*, 2008, vol. 3, no. 1, pp. 19–23.
4. Ivanisenko, Yu., MacLaren, I., Souvage, X., Valiev, R.Z., and Fecht, H.J., Shear-induced $\alpha \to \gamma$ transformation in nanoscale Fe–C composite, *Acta Mater.*, 2006, vol. 54, pp. 1659–1669.
5. Ning, J.-L., Courtois-Manara, E., Kurmanaeva, L., Ganeev, A.V., Valiev, R.Z., Kübel, C., and Ivanisenko, Yu., Tensile properties and work hardening behaviors of ultrafine grained carbon steel and pure iron processed by warm high pressure torsion, *Mater. Sci. Eng., A*, 2013, vol. 581, pp. 8–15.
6. Gavriljuk, V.G., Decomposition of cementite in pearlitic steel due to plastic deformation, *Mater. Sci. Eng., A*, 2003, vol. 345, nos. 1–2, pp. 81–89.
7. Li, Y.J., Chai, P., Bochers, C., Westerkamp, S., Goto, S., Raabe, D., and Kirchheim, R., Atomic-scale mechanisms of deformation-induced cementite decomposition in pearlite, *Acta Mater.*, 2011, vol. 59, no. 10, pp. 3965–3977.
8. Gavriljuk, V.G., Effect of interlamellar spacing on cementite dissolution during wire drawing of pearlitic steel wires, *Scr. Mater.*, 2001, vol. 45, no. 12, pp. 1469–1472.
9. Sheinman, E., Wear of rails. A review of the American press, *J. Frict. Wear*, 2012, vol. 33, no. 4, pp. 308–314.
10. Anisimov, P.S., Influence of design and parameters of trolleys on wear of wheels and rails, *Zheleznodorozhn. Transp.*, 1999, no. 6, pp. 38–42.
11. Gromov, V.E., Yuriev, A.A., Ivanov, Yu.F., et al., Defect substructure change in 100-m differentially hardened rails in long-term operation, *Mater. Lett.*, 2017, vol. 209, pp. 224–227.
12. Gromov, V.E., Yuriev, A.A., Peregudov, O.A., et al., Physical nature of structure and properties degradation of rail surface after long term operation, *AIP Conf. Proc.*, 2017, vol. 1909, p. 020066.
13. Influence of rail wear and lubrication on interaction of vehicle-rail, *Zhelezn. Dorogi Mira*, 2003, no. 9, pp. 66–70.
14. Ermakov, V.M., Analysis of road performance in order to reduce "wheel-rail wear," *Zheleznodorozhn. Transp.*, 2005, no. 7, pp. 58–64.

15. Lysyuk, V.S., The reasons of cars coming-off and rail wear in curves, *Zheleznodorozhn. Transp.*, 2004, no. 11, pp. 50–52.

16. Shapovalov, V.V., Shcherbak, P.N., Maiba, I.A., and Kostygov, V.T., Methods of elimination of wheels and rails wear, *Zheleznodorozhn. Transp.*, 2004, no. 3, pp. 111–115.

17. Grebe, M., Ways to reduce wheel and rail wear, *Zhelezn. Dorogi Mira*, 2002, no. 4, pp. 65–72.

18. Zhong, W., Hu, J.J., Shen, P. Wang, C.Y., and Lius, Q.Y., Experimental investigation between rolling contact fatigue and wear of high-speed and heavy-haul railway and selection of rail material, *Wear*, 2011, vol. 271, nos. 9–10, pp. 2485–2493.

19. Tyfour, W.R., Beynon, J.H., and Kapoor, A., The steady state wear behavior of pearlitic rail steel under dry rolling-sliding contact conditions, *Wear*, 1995, vol. 180, nos. 1–2, pp. 79–89.

20. Singh, U.P. and Singh, R., Wear investigation of wheel and rail steels under conditions of sliding and rolling-sliding contact with particular regard to microstructural parameters, *Wear*, 1993, vol. 170, no. 1, pp. 93–99.

21. *Defekty rel'sov. Klassifikatsiya, katalog i parametry defektnykh i ostrodefektnykh rel'sov* (Rail Defects: Classification, Catalog and Parameters of Cropped and Defective Rails), Moscow: Ross. Zhelezn. Dorogi, 2014.

Translated by O. Polyakov

SPELL: 1. ok